

# CameraMaster: Unified Camera Semantic-Parameter Control for Photography Retouching

Qirui Yang<sup>1,2\*</sup> Yang Yang<sup>2</sup> Ying Zeng<sup>2</sup> Xiaobin Hu<sup>3</sup> Bo Li<sup>2</sup> Huanjing Yue<sup>1</sup>  
 Jingyu Yang<sup>1†</sup> Peng-Tao Jiang<sup>2†</sup>  
<sup>1</sup>Tianjin University <sup>2</sup>vivo Mobile Communication Co., Ltd <sup>3</sup>NUS

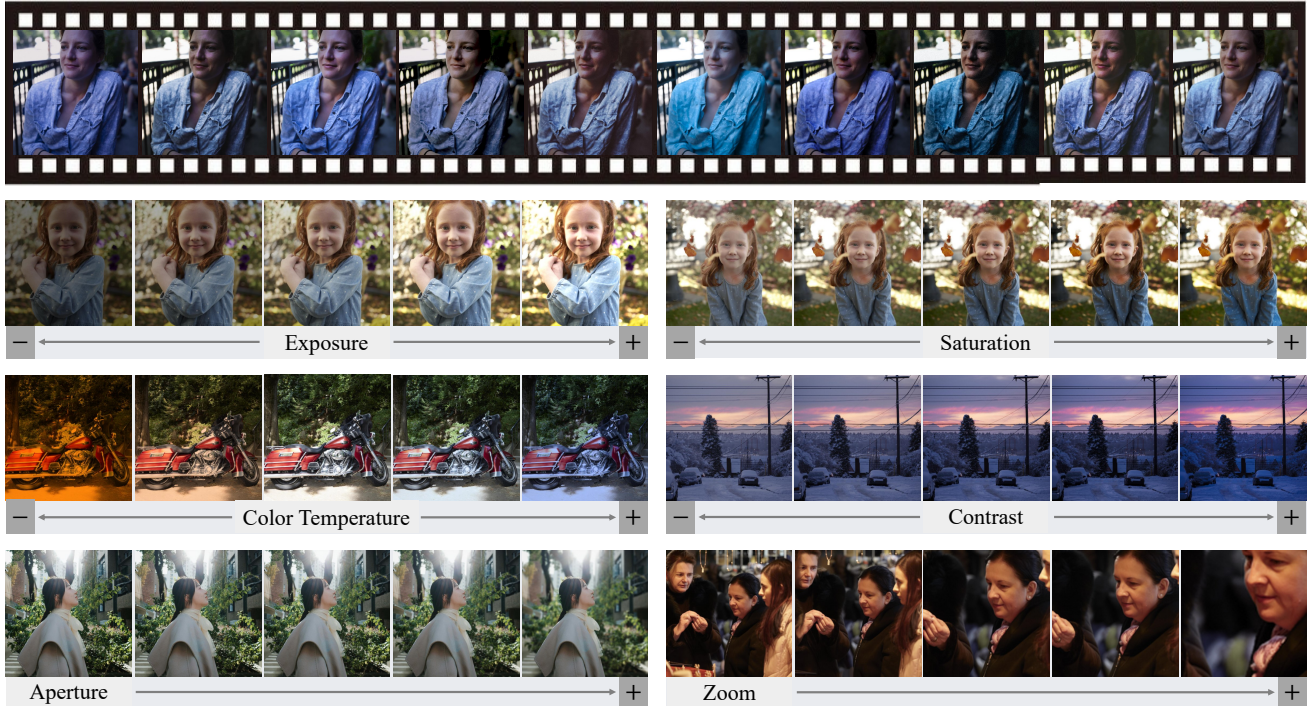


Figure 1. **CameraMaster**: Unified, monotonic, and near-linear photography control. Our framework enables precise, physically consistent retouching across seven key camera dimensions, setting a new benchmark for controllable image retouching.

## Abstract

Text-guided diffusion models have greatly advanced image editing and generation. However, achieving physically consistent image retouching with precise parameter control (e.g., exposure, white balance, zoom) remains challenging. Existing methods either rely solely on ambiguous and entangled text prompts, which hinders precise camera control, or train separate heads/weights for parameter adjustment, which compromises scalability, multi-parameter composition, and sensitivity to subtle variations. To address these limitations, we propose **CameraMaster**, a unified camera-aware framework for image retouching. The key idea is to

explicitly decouple the camera directive and then coherently integrate two critical information streams: a directive representation that captures the photographer’s intent, and a parameter embedding that encodes precise camera settings. **CameraMaster** first uses the camera parameter embedding to modulate both the camera directive and the content semantics. The modulated directive is then injected into the content features via cross-attention, yielding a strongly camera-sensitive semantic context. In addition, the directive and camera embeddings are injected as conditioning and gating signals into the time embedding, enabling unified, layer-wise modulation throughout the denoising process and enforcing tight semantic-parameter alignment. To train and evaluate **CameraMaster**, we construct a large-scale dataset of **78K** image-prompt pairs annotated with camera parameters.

\*Work was done when Qirui Yang was an intern at vivo.

†Corresponding authors.

*Extensive experiments show that CameraMaster produces monotonic and near-linear responses to parameter variations, supports seamless multi-parameter composition, and significantly outperforms existing methods.*

## 1. Introduction

*"A photographer must choose his palette like a painter chooses his palette."—Joel Sternfield*

Image retouching [1–3] is fundamental to modern photography. It allows users to manipulate tone, exposure, color temperature, saturation, and other camera-related attributes with precision to enhance emotional expression and atmospheric rendering in photographic works. However, achieving such fine-grained control remains highly challenging.

Traditional image retouching methods [4–6] typically support only one-to-one mapping for fixed tasks and parameters. They struggle to jointly adjust multiple camera settings, as shown in Fig. 1, which severely limits style diversity, multi-parameter control, and scene generalization. Diffusion-based generative models [7–10] and text-guided multimodal large models [11, 12] provide powerful text-driven editing for general scenarios, but remain inadequate for precise image retouching. For directives such as *increase exposure* or *lower color temperature*, these methods often produce ambiguous, non-monotonic responses that may compromise content fidelity. Overall, both traditional methods and modern generative models lack a precise understanding of camera directives and rigorous modeling of camera parameters. This gap has shifted research focus from merely pursuing photo-realistic fidelity to achieving predictable, controllable image retouching that explicitly corresponds to camera settings.

Recently, several studies [13–17] have integrated physical camera signals into generative modeling. They utilize camera trajectories or viewpoint prompts [18, 19] to achieve controllable perspective synthesis, or leverage the bokeh strength in the textual instruction [20] to adjust depth-of-field effects. However, these methods often treat camera parameters as discrete labels or independent regression targets, rather than modeling them as continuous and monotonic control variables in a unified representation space. For example, [14] adopts differential data, performing differential operations on a set of camera parameter values under the same setting. This encourages the model to focus on inter-image differences, yielding smoother and more consistent generation. However, constrained by a single setting, such methods usually require separate weights for each parameter configuration. This design severely compromises scalability and cross-parameter compositionality. In summary, existing methods fail to provide continuous, monotonic, and physically consistent responses for joint control of multiple camera parameters in a single unified model.

Consequently, achieving robust, precise, and physically consistent camera control remains challenging for three main

reasons: (i) **Lack of camera parameter perception.** Current text encoders in diffusion models [21, 22] tend to understand camera settings as coarse semantic concepts rather than precise quantitative variables. This leads to editing results that lack continuity, monotonicity, and physical fidelity. (ii) **Entanglement between camera directives and content semantics.** Although text encoders [23–25] are powerful, they struggle to cleanly separate camera control intents from mixed prompts. Simply concatenating camera control text with content descriptions often causes brief camera-related semantics to be overwhelmed by strong content semantics. (iii) **Absence of a unified, scalable framework.** Existing methods [14, 20, 26] typically train separate heads/weights or even independent models for each parameter. This results in fragmented interfaces and reduced sensitivity to parameter combinations and subtle variations. These limitations motivate us to develop a unified, scalable, and physically consistent framework for camera-aware image retouching.

To address these challenges, we propose **CameraMaster**, a unified framework for camera-aware image retouching. CameraMaster adopts a dual-branch architecture that separately models semantic information and physical camera parameters, realizing parameter-aware and semantic disentanglement, ensuring precise perception and responsive control. Specifically, we divide the information flow into two branches: a *semantic stream*, which encodes camera directives and content descriptions, and a *parameter stream*, which encodes explicit and quantifiable camera parameters. To enhance parameter awareness, the parameter stream maps camera parameter values into compact parameter embeddings. These parameter embeddings then modulate the semantic stream and time embedding, allowing each component of the model to perceive and respond to precise camera parameters. To mitigate semantic entanglement, we separately encode the camera directive representation and the content semantic representation, and fuse them through cross-attention, forming a unified semantic feature that is highly sensitive to camera directives. This unified semantic feature is injected into the DiT backbone to condition generation. Through separate encoding and interaction between semantic and parameter streams, CameraMaster establishes a robust paradigm for camera-awareness image retouching. Furthermore, we construct a camera-aware retouching dataset of **78K** image–prompt pairs annotated with professional camera parameters for model training and evaluation. Experimental results demonstrate that our method produces monotonic and near-linear responses to parameter variations and achieves superior performance against other baselines in controllable image retouching. In general, our contributions to the community are threefold:

- We propose CameraMaster, a unified framework that achieves monotonic and continuous image retouching through professional camera parameters.

- We design a decoupling and fusion mechanism that effectively separates camera parameters from camera directives, ensuring precise perception and responsive control.
- We construct a dataset of 78K image–prompt pairs annotated with camera parameters, enabling supervised alignment between semantic and parametric spaces.

## 2. Related Work

### 2.1. Image Retouching and Enhancement

LUT-based methods model color grading as Look-up Tables [1, 4, 6, 27], often blending multiple base LUTs with content-dependent weights to approximate professional tone curves [28–33]. While efficient and easy to deploy, these methods are largely image-independent, limited in dynamic range, and struggle to realize local, content-aware behaviors, which constrain faithful reproduction of subtle photographic adjustments. Learning-based methods [34–36] address these issues with end-to-end optimization and structured representations. HDRNet [37] introduced a bilateral grid representation for fast local tone mapping. Deep 3D LUTs [4] and SepLUT [38] learned parameterized color transforms from annotated data. LPTN [39] used Laplacian pyramids to preserve high-frequency detail, and DPRNet [3] proposed a differential pyramid representation for high-fidelity retouching. These methods demonstrate outstanding performance in one-to-one feature mapping, but they only support fixed tasks and parameters, severely limiting their capabilities for multi-task, multi-parameter adjustment, and scene generalization. They lack explicit correlation with multi-camera parameters (such as exposure, white balance, and aperture), prompting research to move beyond fine-grained single retouching toward unified image retouching and editing.

### 2.2. Generative and Photographic Image Editing

Classical editing pipelines relied on explicit pixel operations and handcrafted filters to control geometric or photometric changes [40–42]. They offered precision but limited semantic awareness and contextual adaptability. Diffusion models enable semantically grounded generation and editing in learned latent spaces [43–46]. Building on this foundation, recent methods support local, context-preserving edits and extend to mask-based or geometry-aware manipulations [7, 8, 11, 26, 47–50]. Instruction-tuned frameworks further adapt diffusion backbones with synthetic instruction–response pairs, and transformer variants improve fidelity and edit consistency on richer data [22, 43, 51, 52]. However, these pipelines operate mainly in the semantic domain. Prompts such as “slightly brighter” or “warmer tone” are intuitive but indirect, often yielding ambiguous, nonlinear, and scene-dependent effects [14, 53]. This semantic–physical gap motivates models that respond deterministically and monotonically to camera parameters, bringing generative editing closer to photographic practice.

### 2.3. Physically-based Photographic Control

A complementary line of work integrates physical camera signals into generative modeling. Some works [18, 19] leverage camera trajectories or depth prompts for controllable viewpoint synthesis, while others condition on aperture or focal distance for limited depth-of-field effects. Yet, most methods [14, 20, 54] treat camera variables as discrete tokens or independent regression targets, rather than continuous, interpretable controls within a unified representation. Moreover, task-specific subnetworks or per-parameter weights, common in current systems for exposure or white balance, undermine scalability, cross-parameter composability, and sensitivity to subtle variations [14, 55, 56]. These limitations point to the need for a single, extensible mechanism that embeds semantic descriptions and numeric magnitudes directly into the generative backbone to achieve stable, monotonic, and disentangled control across photographic factors. Our work departs from these paradigms by introducing a unified, all-in-one framework that explicitly models the semantic–numeric duality of photographic parameters, thereby aligning the convenience of text-driven editing with the determinism of camera-level control.

## 3. Method

### 3.1. Overview

In this paper, we aim to achieve scalable, robust, and physically consistent camera control for photography retouching. As shown in Fig. 2, we propose **CameraMaster**, a unified framework for camera-aware image retouching built on a diffusion transformer (DiT) backbone. The model receives three inputs: the input image, an image content description  $c$  (caption), and a structured camera control directive  $d$  (creative intent). The core of our framework is how to decouple and interact with semantic information and camera parameters – containing camera directives, image content, and directive parameters – to obtain semantic embeddings that are sensitive to camera directives and parameters. To this end, we adopt a two-branch architecture: a *semantic stream* and a *parameter stream*. The semantic stream encodes a directive representation from the camera directive  $d$  and a content semantic representation from the content description  $c$ . These representations are then modulated and fused to produce a unified, camera-aware semantic embedding that serves as the main textual guidance for DiT. The parameter stream extracts precise numerical values from the camera directive  $d$  and encodes them into compact camera parameter embeddings. The effectiveness of CameraMaster lies in the interaction between these two streams: camera parameter embeddings conditionally modulate the semantic stream, ensuring that the fusion of directives and content is physically grounded and accurately reflects numerical settings. In addition, the parameter embedding is injected into

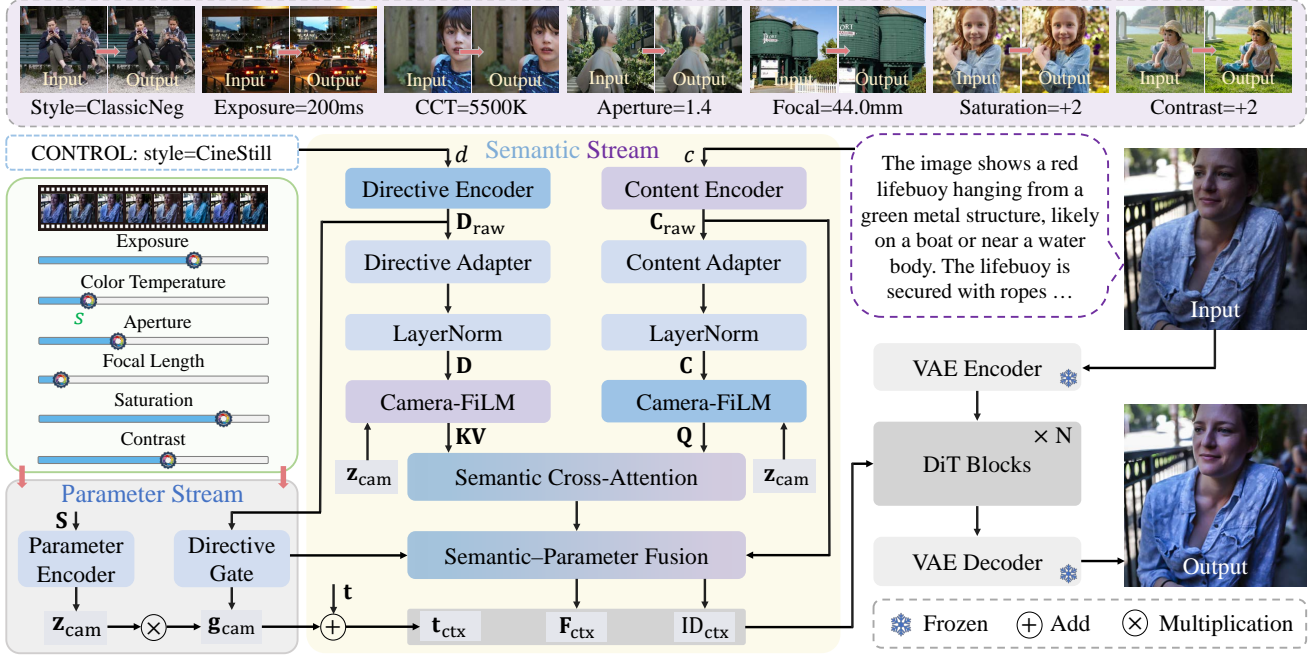


Figure 2. **Pipeline of CameraMaster for image retouching.** Given an input image, a camera directive  $d$  and a content description  $c$ , CameraMaster decouples control into two streams: a *semantic stream* that encodes  $d$  and  $c$ , and a *parameter stream* that parses the directive into a calibrated camera vector  $s$  and its embedding  $z_{\text{cam}}$ . The parameter embedding  $z_{\text{cam}}$  modulates both the semantic representations ( $C_{\text{raw}}$ ,  $D_{\text{raw}}$ ) and the time embedding  $t$ , providing explicit parameter awareness. The modulated features are fused into a unified semantic context and injected into the DiT backbone, enabling continuous, monotonic, and physically consistent camera control for image retouching.

the DiT backbone by modulating the time embedding. This dual-path design, where semantic information is physically modulated before guiding the model, while physical parameters provide direct global guidance, enables CameraMaster to achieve robust, continuous, and predictable control.

### 3.2. Decoupled Representations

To avoid semantic ambiguity and ensure precise control, CameraMaster decouples control signals into two independent information streams. For the semantic stream, we employ two pretrained text encoders [23, 24] to encode guided text into semantic representations. Given the camera control directive  $d$  (e.g., “[CONTROL: style=CineStill]”) and the image content description  $c$ , the encoders generate two high-dimensional semantic representations:

$$D_{\text{raw}} = \text{Encoder}_{\text{SigLIP}}(d), \quad C_{\text{raw}} = \text{Encoder}_{\text{T5}}(c), \quad (1)$$

where  $D_{\text{raw}}$  captures the photographer’s intent and  $C_{\text{raw}}$  anchors the scene content. To enable adaptive control strength during subsequent fusion, we further predict a camera directive gate  $g_{\text{cam}} \in (0, 1)$  from  $D_{\text{raw}}$  to capture the relative importance of the directive.

In parallel, the parameter stream extracts and quantifies precise camera settings. To obtain near-linear, monotonic responses, we design a parameter-aware parsing and calibration pipeline that converts free-form values extracted from

directives (e.g., “CineStill”) into physically meaningful normalized scalars. For example, exposure is represented as a shutter ratio relative to a reference time; color temperature is transformed using logarithmic scaling and normalized; ordinal levels (e.g., contrast) are linearly mapped to  $[-1, 1]$ ; and discrete styles are one-hot encoded and then mapped to  $[0, 1]$ . This calibration step is crucial for achieving physical consistency. After parsing and normalization, we obtain a calibrated camera parameter vector  $s$ . *More details are provided in Section 4.1.*

To encode the camera parameter vector into a compact camera parameter embedding, we first broadcast  $s$  into a multi-channel camera parameter tensor  $S \in \mathbb{R}^{B \times 3 \times H \times W}$ , whose spatial dimensions match the input image size. We then introduce a conditional network that encodes the camera parameter tensor into a compact embedding  $z_{\text{cam}}$ . This conditional network consists of four convolutional layers, an adaptive average pooling layer, and an MLP layer. In this way, we decouple the input signal into two independent, high-dimensional representations: semantic representations ( $D_{\text{raw}}$ ,  $C_{\text{raw}}$ ) and a camera parameter embedding ( $z_{\text{cam}}$ ), which form the basis for subsequent collaborative fusion.

### 3.3. Parameter Modulation and Semantic Fusion

Given the effective decoupling of semantic and parameter information, the next key challenge is their modulation and fusion. To enable semantic representations to perceive precise

camera values and yield monotonic, near-linear responses, we design a camera parameter feature-wise linear modulation, referred to as Camera-FiLM.

To facilitate modulation, we first align the dimensions of the content semantic representation  $\mathbf{C}_{\text{raw}}$  and the camera directive representation  $\mathbf{D}_{\text{raw}}$  using a camera adapter and a content adapter:

$$\mathbf{D} = \text{Adapter}_{\text{dir}}(\mathbf{D}_{\text{raw}}), \quad \mathbf{C} = \text{Adapter}_{\text{con}}(\mathbf{C}_{\text{raw}}), \quad (2)$$

where each Adapter module consists of a linear layer, a softmax operation, and a LayerNorm layer.

Camera-FiLM then dynamically generates affine transformation parameters (scaling  $\gamma$  and bias  $\beta$ ) from  $\mathbf{z}_{\text{cam}}$ :

$$\gamma_q, \beta_q = \text{FiLM}_q(\mathbf{z}_{\text{cam}}), \quad \gamma_{kv}, \beta_{kv} = \text{FiLM}_{kv}(\mathbf{z}_{\text{cam}}). \quad (3)$$

These affine parameters modulate the two semantic representations as

$$\mathbf{Q} = (1 + \gamma_q) \odot \mathbf{C} + \beta_q, \quad \mathbf{K}, \mathbf{V} = (1 + \gamma_{kv}) \odot \mathbf{D} + \beta_{kv}. \quad (4)$$

To address semantic ambiguity and prevent the directive signal from being overwhelmed by strong content semantics, we design a semantic cross-attention module that injects the camera directive representation into the content semantic representation:

$$\mathbf{C}_{\text{fuse}} = \text{Softmax}\left(\frac{\mathbf{Q}\mathbf{K}^\top}{\sqrt{d_K}}\right)\mathbf{V}, \quad (5)$$

where  $d_K$  denotes the dimensionality of  $\mathbf{K}$ . This encourages the content semantic representation to be highly sensitive to the camera directive representation.

We further introduce an adaptive gating mechanism that modulates the strength of the residual connection using the camera directive gate  $\mathbf{g}_{\text{cam}}$ :

$$\mathbf{C}_{\text{ctx}} = \mathbf{C}_{\text{raw}} + \mathbf{g}_{\text{cam}} \cdot \mathbf{C}_{\text{fuse}}. \quad (6)$$

The resulting  $\mathbf{C}_{\text{ctx}}$  forms our unified semantic feature, which integrates camera directive intent, content semantics, and camera parameters.

### 3.4. Semantic-Parameter Information Injection

To achieve robust, multi-faceted control, we inject camera information into the DiT through a dual-pathway mechanism. This design provides the model with both a rich fused semantic context and a direct physical conditioning signal for global modulation.

Although  $\mathbf{C}_{\text{ctx}}$  provides a holistic semantic context, the fusion process can dilute the salience of individual control directives across many tokens. To preserve explicit control, we complement the fused context with an addressable camera directive representation. Specifically, we compress the

original camera directive representation  $\mathbf{D}$  with two linear layers to obtain a compact camera directive context  $\mathbf{D}_{\text{dir}}$ . We then concatenate this with the fused context to form the full semantic input  $\mathbf{F}_{\text{ctx}}$ :

$$\mathbf{F}_{\text{ctx}} = \text{Concat}(\mathbf{C}_{\text{ctx}}, \mathbf{g}_{\text{cam}} \cdot \mathbf{D}_{\text{dir}}), \quad (7)$$

where the camera directive gate  $\mathbf{g}_{\text{cam}}$  controls the contribution of the explicit directive. By providing both the blended context  $\mathbf{C}_{\text{ctx}}$  and the camera directive context  $\mathbf{D}_{\text{dir}}$ , we enable the DiT’s attention mechanism to learn the overall camera control.

To further enhance fine-grained control, we provide explicit positional information by concatenating the positional encodings for the content and the camera directive:

$$\mathbf{ID}_{\text{ctx}} = \text{Concat}(\mathbf{ID}_{\text{content}}, \mathbf{ID}_{\text{dir}}), \quad (8)$$

where  $\mathbf{ID}_{\text{content}}$  denotes the standard sequential indices for the content tokens and  $\mathbf{ID}_{\text{dir}}$  is assigned a new block of continuous integer indices that follow the last content index. This creates a unified, unambiguous positional map for the entire input sequence.

In this way, the DiT learns not only what the control is, but also where its semantic representation is located, enabling more precise and disentangled retouching. Furthermore, the camera parameter embedding  $\mathbf{z}_{\text{cam}}$  modulates the time embedding  $\mathbf{t}$ :

$$\mathbf{t}_{\text{ctx}} = \mathbf{t} + \mathbf{g}_{\text{cam}} \cdot \psi(\mathbf{z}_{\text{cam}}), \quad (9)$$

where  $\psi$  is a two-layer MLP. The modulated embedding  $\mathbf{t}_{\text{ctx}}$  conditions all AdaLN layers within the DiT blocks. Through this architecture, CameraMaster closely aligns semantic intentions with physical parameter values, achieving precise, composable, and physically coherent control.

## 4. Experiments

### 4.1. Dataset: CameraSet

**Goal and Scope.** To support monotonic, continuous, and fine-grained photo retouching, we construct a large-scale dataset, **CameraSet**, specifically designed for real-world camera-aware retouching. CameraSet selects 2K images from the FilmSet dataset [5] as base images, with wide dynamic range, appropriate exposure, and neutral color temperature. On top of these, we physically simulate multiple camera functions, including film style, color temperature, exposure, zoom, contrast, saturation, and bokeh. Each function comprises multiple quantifiable parameter settings analogous to real camera controls.

We categorize CameraSet into several calibrated settings: (i) *Film Simulation*: To support emotional expression and atmospheric rendering, we employ multiple photographers to meticulously simulate various classic film styles. **10** iconic

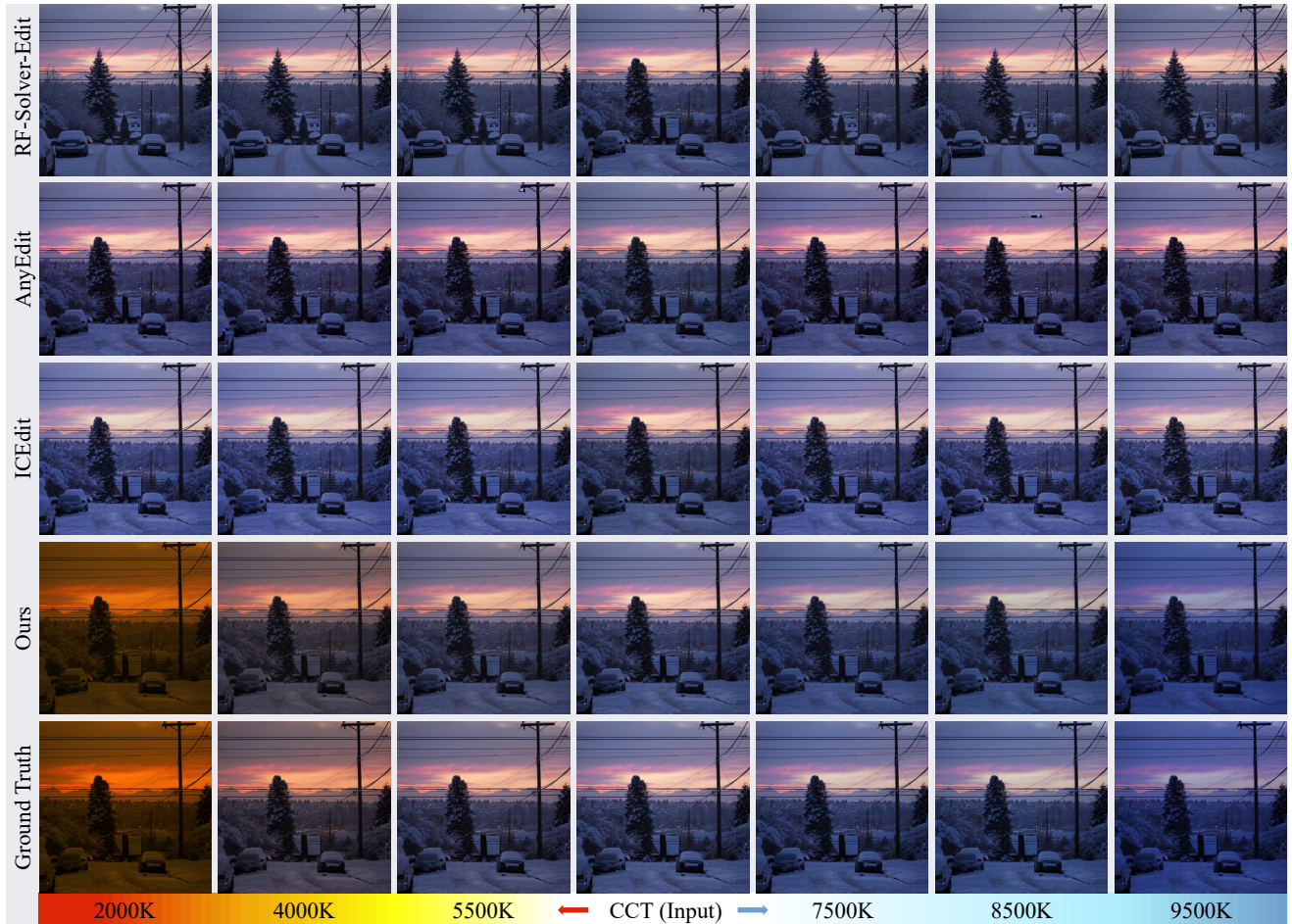


Figure 3. Visual comparison of Color Temperature (CCT) task retouching results across different methods. This method achieves continuous, monotonous, and precise control over retouching intensity, which strikes a balance between following directions and preserving the original image’s consistency to meet user needs.

films (such as ClassicNeg, Velvia, Kodak Gold, etc.) are selected to offer diverse options. (ii) *Exposure*: We adjust the irradiance of the base image and convert it back to RGB using a simulated image signal processor (ISP) [14, 57], producing images with different exposure levels. (iii) *Color Temperature*: We use an empirical approximation [58] based on the relationship between blackbody radiation and color temperature to adjust RGB channel ratios for different color temperatures. (iv) *Contrast and Saturation*: We synthesize four levels of contrast and saturation using Photoshop, covering common retouching ranges. (v) *Zoom*: We follow end-to-end methods [14, 59, 60]. For each base image, we compute the field-of-view (FoV) ratio corresponding to a sampled focal length relative to the original focal length. (vi) *Bokeh*: We construct 400 base–foreground pairs and render four levels of blur to simulate different apertures and subject distances [54].

All values are normalized into a standard camera vector  $s$  (see Section 3.2), ensuring that equal text strides correspond

to equal numerical strides across different control parameters, consistent with the pre-attention conditioning setup.

**Pair Generation and Calibration.** For each base image, we generate input–output pairs by applying physically driven parametric operations. Each data point is annotated with: (a) a *camera control directive*  $d$ , and (b) a content description  $c$  (image caption) describing the image, generated by a vision–language model [61]. This pairing aligns semantic intent with numerical targets and forms the basis for evaluating monotonic control curves.

**Dataset Details** CameraSet provides 2,000 training pairs per control parameter, for a total of **78K** training pairs. For evaluation, CameraSet includes **570** test pairs. The test set is disjoint from the training set and covers all control parameters, enabling assessment of continuity, monotonicity, and identity preservation under controlled editing conditions. To further evaluate CameraMaster’s generalization in real-world scenarios, we also collect an additional dataset of real scenes without paired ground truth.



Figure 4. Examples showcase the cross-parameter retouching power of CameraMaster on the real-world dataset. Our method allows for continuous and fine-grained retouching across multiple parameter combinations, illustrating CameraMaster’s universal capability in achieving diverse retouching objectives.

Table 1. **Quantitative results on CameraSet test set.** All metrics are calculated between the retouching image and the ground truth image provided by the CameraSet.

Methods	PSNR $\uparrow$	SSIM $\uparrow$	LPIPS $\downarrow$	PDist $\downarrow$	$\Delta E$ $\downarrow$	CLIP-I $\uparrow$	DINO $\uparrow$	FID $\downarrow$
RF-Solver-Edit* [68]	19.68	0.7332	0.3556	15.03	10.38	0.8719	0.8354	93.64
FLUX.1 Fill* [25]	10.19	0.3708	0.7733	23.03	25.90	0.6480	0.4836	202.53
FLUX.1 Kontext* [69]	11.91	0.4262	0.6807	22.42	23.93	0.7826	0.7014	115.48
InstructP2P [43]	26.47	0.8002	0.1319	12.96	4.40	0.9643	0.9478	30.46
OminiControl [70]	14.72	0.6026	0.5241	17.90	16.18	0.7533	0.6921	140.25
AnyEdit [21]	25.48	0.7871	0.1572	12.44	4.89	0.9383	0.8854	37.63
ICEdit [22]	23.57	0.8079	0.2209	10.91	9.15	0.9266	0.9370	31.50
<b>CameraMaster</b>	<b>32.80</b>	<b>0.9240</b>	<b>0.0669</b>	<b>5.66</b>	<b>3.07</b>	<b>0.9846</b>	<b>0.9865</b>	<b>7.70</b>

## 4.2. Implementation Details

We train our model using the AdamW optimizer with a learning rate of  $5 \times 10^{-4}$ . The training resolution is set to  $1024 \times 1024$ . All experiments are conducted on 8 NVIDIA H20 GPUs. To comprehensively evaluate our model, we compute PSNR, SSIM, LPIPS [62], PDist,  $\Delta E$  [63], CLIP-I [64, 65], DINO [66], and FID [67] metrics to measure the discrepancy between model outputs and ground truth.

## 4.3. Comparisons with State-of-the-Art

**Quantitative Comparison.** To evaluate CameraMaster’s performance, we quantitatively compared it against a suite of state-of-the-art image editing methods on our constructed CameraSet test dataset. The benchmark methods span multiple paradigms, including off-the-shelf powerful training-free universal editors (RF-Solver-Edit [68], FLUX.1 [25], FLUX.1 Kontext [69]) and retrained instruction-driven editing models (InstructP2P [43], OminiControl [70], AnyEdit [21], ICEdit [22]). As shown in Tab. 1, CameraMaster significantly outperforms all baseline methods across all 8 evaluation metrics, achieving state-of-the-art performance. This

demonstrates the effectiveness of our framework for precise, physically consistent image retouching. In particular, CameraMaster shows clear advantages in reconstruction fidelity and perceptual quality. CameraMaster achieves 32.80 dB in terms of PSNR metric, surpassing the strongest baseline method, InstructP2P, by 6.33 dB. Moreover, CameraMaster’s LPIPS score is only 0.0669. Regarding color accuracy, the  $\Delta E$  metric reached 3.07, significantly outperforming all competitors. This success stems directly from our decoupled semantic and parameter stream, which provides precise numerical guidance to the model, eliminating the ambiguity inherent in pure text instructions.

Furthermore, in terms of content and semantic consistency, the CLIP-I and DINO scores (0.9846 and 0.9865, respectively) both rank first. This demonstrates that CameraMaster maximally preserves the original image’s content and identity characteristics while executing precise camera parameter adjustments, effectively avoiding the “content drift” or identity destruction issues common in other methods.

To further validate and evaluate CameraMaster, especially in more challenging real-world scenarios lacking ground

Table 2. **Quantitative results on real-world dataset.**

Settings	CLIP-DIST $\uparrow$	CLIP-SIM $\uparrow$	DINO-DIST $\downarrow$	DINO-SIM $\uparrow$
RF-Solver-Edit	0.0889	0.9111	0.1154	0.8846
FLUX.1 Fill	0.2969	0.7031	0.4755	0.5245
InstructP2P	0.0971	0.9029	0.0725	0.9275
OminiControl	0.2174	0.7827	0.1860	0.8140
AnyEdit	0.0751	0.9248	0.0623	0.9377
ICEdit	0.0674	0.9325	0.0363	0.9636
Ours	<b>0.0293</b>	<b>0.9707</b>	<b>0.0184</b>	<b>0.9816</b>

truth benchmarks, we have conducted additional experiments. As shown in Tab. 2, our model achieves state-of-the-art performance across all relevant metrics, including the lowest CLIP-DIST and DINO-DIST, as well as the highest CLIP-SIM and DINO-SIM. The achievement stems from our parameter modulation and semantic fusion mechanism. Finally, CameraMaster achieved a decisive victory in the photorealism and distributional quality of generated images.

In summary, quantitative comparisons unequivocally validate the design advantages of the CameraMaster framework. Compared to generic editing models reliant on ambiguous semantic instructions, our approach successfully establishes a new technical benchmark across all critical dimensions of image retouching—precision, fidelity, content preservation, and photorealism—by decoupling semantic intent from camera parameters and efficiently aligning them.

**Qualitative Results.** As shown in Fig. 3, the results show a qualitative comparison on the color temperature (CCT) task. When we gradually vary the CCT value, CameraMaster produces smooth and monotonic changes in global color tone, while preserving scene structure and local details. In contrast, diffusion-based baselines often exhibit non-monotonic shifts and or failures. These results confirm that semantic-parameter alignment enables precise, continuous control of retouching strength and maintains a good balance between following camera directives and keeping the original content intact. As shown in Fig. 4, CameraMaster operates on real images with joint control of multiple parameters (e.g., exposure, saturation, style). Our method supports fine-grained, continuous transitions across different parameter combinations, yielding coherent and natural retouching results while preserving identity and scene layout. Compared with baselines, CameraMaster better respects each target parameter dimension and avoids unintended changes, highlighting its generality and practicality for diverse, camera-centric retouching goals. *More qualitative results can be found in the supplementary materials.*

#### 4.4. Ablation Study

We conducted ablation experiments to validate the effectiveness of key components in our CameraMaster framework. All experiments were performed on the CameraSet test dataset, with results shown in Tab. 3. We first established a baseline model that removed our decoupled design,

Table 3. **Ablation study on model structure.** We evaluate the performance of different settings on the CameraSet test set.

Settings	PSNR $\uparrow$	SSIM $\uparrow$	LPIPS $\downarrow$	$\Delta E$ $\downarrow$
Training-free	11.91	0.4262	0.6807	23.93
Benchmark	28.54	0.9203	0.0599	0.981
w/o Parametric	30.68	0.9237	0.0541	3.182
w/o Semantic	31.27	0.9145	0.0856	3.902
Full model	<b>32.80</b>	<b>0.9240</b>	<b>0.0669</b>	<b>3.073</b>

directly feeding text prompts with camera parameters into the text encoder. Concurrently, we included an off-the-shelf benchmark [69] to demonstrate the necessity of fine-tuning. Our complete model significantly outperforms the baseline across all key metrics. Particularly on the PSNR metric, our model achieves 32.80 dB, surpassing the baseline (28.54 dB) by 4.26 dB. This strongly demonstrates that simply concatenating semantic and parametric information in text is a suboptimal strategy, while our proposed architecture more effectively leverages both types of information to achieve higher-fidelity image retouching.

In the *w/o Parametric setting*, we removed the camera parameter stream. Experimental results show PSNR significantly dropped from 32.88 dB to 30.68 dB. This substantial performance degradation indicates that camera parameter embeddings are crucial for achieving pixel-level precise reconstruction. In the *w/o Semantic setting*, we removed the semantic stream, allowing the model to receive only calibrated physical parameter vectors without knowing which specific camera parameters these values correspond to. Under these conditions, the model’s performance also deteriorated across the board, particularly in perceptual metrics LPIPS (degrading from 0.0669 to 0.0856) and color accuracy  $\Delta E$  (worsening from 3.073 to 3.902). This demonstrates that camera instruction representations provide indispensable contextual information for camera parameters. Without semantic instruction guidance, the model struggles to correctly interpret and apply these numerical values, leading to perceptual and color deviations in the generated results. An intriguing phenomenon is that despite the baseline model’s overall poor performance, its  $\Delta E$  metric is unusually good. Our analysis suggests this occurs because it fails to effectively interpret complex editing instructions, instead tending to execute very conservative, minimal edits. While this failure mode causes minimal color disturbance, it completely fails to accomplish the intended retouching task, as evidenced by its extremely low PSNR values.

## 5. Conclusion

In this paper, we introduce **CameraMaster**, a unified framework for camera-aware photographic retouching. Our key idea is to explicitly separate control signals into two information streams: a stream for photographic instruction repre-

sentations and a stream for camera parameter embeddings that encode precise numerical settings. Through tailored modulation, cross-attention, and unified injection mechanisms, CameraMaster effectively aligns and fuses these two streams within a single diffusion-based model. We conduct extensive experiments on a newly constructed dataset of 78K image–prompt pairs with camera parameter annotations. Experimental results demonstrate that our method produces monotonic and near-linear responses to parameter variations and achieves superior performance against other baselines in controllable image retouching.

## References

- [1] Feng Zhang, Ming Tian, Zhiqiang Li, Bin Xu, Qingbo Lu, Changxin Gao, and Nong Sang. Lookup table meets local laplacian filter: pyramid reconstruction network for tone mapping. *Advances in Neural Information Processing Systems*, 36:57558–57569, 2023. 2, 3
- [2] Wanchao Su, Can Wang, Chen Liu, Fangzhou Han, Hongbo Fu, and Jing Liao. Styleretoucher: Generalized portrait image retouching with gan priors. *IEEE Transactions on Visualization and Computer Graphics*, 2024.
- [3] Qirui Yang, Yinbo Li, Peng-Tao Jiang, Qihua Cheng, Biting Yu, Yihao Liu, Huanjing Yue, and Jingyu Yang. Learning differential pyramid representation for tone mapping. *arXiv preprint arXiv:2412.01463*, 2024. 2, 3
- [4] Hui Zeng, Jianrui Cai, Lida Li, Zisheng Cao, and Lei Zhang. Learning image-adaptive 3d lookup tables for high performance photo enhancement in real-time. *IEEE Transactions on Pattern Analysis and Machine Intelligence*, page 1–1, Jan 2020. 2, 3
- [5] Zinuo Li, Xuhang Chen, Shuqiang Wang, and Chi-Man Pun. A large-scale film style dataset for learning multi-frequency driven film enhancement. In *IJCAI*, pages 1160–1168, 2023. 5
- [6] Kang Fu, Yicong Peng, Zicheng Zhang, Qihang Xu, Xiaohong Liu, Jia Wang, and Guangtao Zhai. Attentionlut: Attention fusion-based canonical polyadic lut for real-time image enhancement. In *ICASSP 2024-2024 IEEE International Conference on Acoustics, Speech and Signal Processing (ICASSP)*, pages 3255–3259. IEEE, 2024. 2, 3
- [7] Robin Rombach, Andreas Blattmann, Dominik Lorenz, Patrick Esser, and Björn Ommer. High-resolution image synthesis with latent diffusion models. In *Proceedings of the IEEE/CVF conference on computer vision and pattern recognition*, pages 10684–10695, 2022. 2, 3
- [8] Andreas Lugmayr, Martin Danelljan, Andres Romero, Fisher Yu, Radu Timofte, and Luc Van Gool. Repaint: Inpainting using denoising diffusion probabilistic models. In *Proceedings of the IEEE/CVF conference on computer vision and pattern recognition*, pages 11461–11471, 2022. 3
- [9] Dar-Yen Chen, Hamish Tennent, and Ching-Wen Hsu. Artadapter: Text-to-image style transfer using multi-level style encoder and explicit adaptation. In *Proceedings of the IEEE/CVF conference on computer vision and pattern recognition*, pages 8619–8628, 2024.
- [10] Yu Zeng, Vishal M Patel, Haochen Wang, Xun Huang, Ting-Chun Wang, Ming-Yu Liu, and Yogesh Balaji. Jedi: Joint-image diffusion models for finetuning-free personalized text-to-image generation. In *Proceedings of the IEEE/CVF Conference on Computer Vision and Pattern Recognition*, pages 6786–6795, 2024. 2
- [11] Lvmin Zhang, Anyi Rao, and Maneesh Agrawala. Adding conditional control to text-to-image diffusion models. In *Proceedings of the IEEE/CVF international conference on computer vision*, pages 3836–3847, 2023. 2, 3
- [12] Nupur Kumari, Bingliang Zhang, Richard Zhang, Eli Shechtman, and Jun-Yan Zhu. Multi-concept customization of text-to-image diffusion. In *Proceedings of the IEEE/CVF conference on computer vision and pattern recognition*, pages 1931–1941, 2023. 2
- [13] Zhenzhi Wang, Yixuan Li, Yanhong Zeng, Youqing Fang, Yuwei Guo, Wenran Liu, Jing Tan, Kai Chen, Tianfan Xue, Bo Dai, et al. Humanvid: Demystifying training data for camera-controllable human image animation. *Advances in Neural Information Processing Systems*, 37:20111–20131, 2024. 2
- [14] Yu Yuan, Xijun Wang, Yichen Sheng, Prateek Chennuri, Xingguang Zhang, and Stanley Chan. Generative photography: Scene-consistent camera control for realistic text-to-image synthesis. In *Proceedings of the Computer Vision and Pattern Recognition Conference*, pages 7920–7930, 2025. 2, 3, 6
- [15] Guangcong Zheng, Teng Li, Rui Jiang, Yehao Lu, Tao Wu, and Xi Li. Cami2v: Camera-controlled image-to-video diffusion model. *arXiv preprint arXiv:2410.15957*, 2024.
- [16] Zhengfei Kuang, Shengqu Cai, Hao He, Yinghao Xu, Hongsheng Li, Leonidas J Guibas, and Gordon Wetzstein. Collaborative video diffusion: Consistent multi-video generation with camera control. *Advances in Neural Information Processing Systems*, 37:16240–16271, 2024.
- [17] Edurne Bernal-Berdun, Ana Serrano, Belen Masia, Matheus Gadelha, Yannick Hold-Geoffroy, Xin Sun, and Diego Gutierrez. PreciseCam: Precise camera control for text-to-image generation. In *Proceedings of the Computer Vision and Pattern Recognition Conference*, pages 2724–2733, 2025. 2
- [18] Dejia Xu, Weili Nie, Chao Liu, Sifei Liu, Jan Kautz, Zhangyang Wang, and Arash Vahdat. Camco: Camera-controllable 3d-consistent image-to-video generation. *arXiv preprint arXiv:2406.02509*, 2024. 2, 3
- [19] Hao He, Yinghao Xu, Yuwei Guo, Gordon Wetzstein, Bo Dai, Hongsheng Li, and Ceyuan Yang. Cameractrl: Enabling camera control for video diffusion models. In *The Thirteenth International Conference on Learning Representations*, 2025. 2, 3
- [20] Armando Fortes, Tianyi Wei, Shangchen Zhou, and Xingang Pan. Bokeh diffusion: Defocus blur control in text-to-image diffusion models. *arXiv preprint arXiv:2503.08434*, 2025. 2, 3
- [21] Qifan Yu, Wei Chow, Zhongqi Yue, Kaihang Pan, Yang Wu, Xiaoyang Wan, Juncheng Li, Siliang Tang, Hanwang Zhang, and Yueting Zhuang. Anyedit: Mastering unified high-quality image editing for any idea. *arXiv preprint arXiv:2411.15738*, 2024. 2, 7

- [22] Zechuan Zhang, Ji Xie, Yu Lu, Zongxin Yang, and Yi Yang. In-context edit: Enabling instructional image editing with in-context generation in large scale diffusion transformer. *arXiv preprint arXiv:2504.20690*, 2025. 2, 3, 7
- [23] Colin Raffel, Noam Shazeer, Adam Roberts, Katherine Lee, Sharan Narang, Michael Matena, Yanqi Zhou, Wei Li, and Peter J Liu. Exploring the limits of transfer learning with a unified text-to-text transformer. *Journal of machine learning research*, 21(140):1–67, 2020. 2, 4
- [24] Xiaohua Zhai, Basil Mustafa, Alexander Kolesnikov, and Lucas Beyer. Sigmoid loss for language image pre-training. In *Proceedings of the IEEE/CVF international conference on computer vision*, pages 11975–11986, 2023. 4
- [25] Black Forest Labs. Flux. <https://github.com/black-forest-labs/flux>, 2024. 2, 7
- [26] Yiren Song, Cheng Liu, and Mike Zheng Shou. Omniconsistency: Learning style-agnostic consistency from paired stylization data. *arXiv preprint arXiv:2505.18445*, 2025. 2, 3
- [27] Jiacheng Li, Chang Chen, Zhen Cheng, and Zhiwei Xiong. Toward dnn of luts: Learning efficient image restoration with multiple look-up tables. *IEEE Transactions on Pattern Analysis and Machine Intelligence*, 2024. 3
- [28] Ke Xu Haoyuan Wang and Rynson W.H. Lau. Local color distributions prior for image enhancement. In *Proceedings of the European Conference on Computer Vision (ECCV)*, 2022. 3
- [29] Haofeng Liu, Heng Li, Huazhu Fu, Ruoxiu Xiao, Yunshu Gao, Yan Hu, and Jiang Liu. Degradation-invariant enhancement of fundus images via pyramid constraint network. In *International Conference on Medical Image Computing and Computer-Assisted Intervention*, pages 507–516. Springer, 2022.
- [30] Yili Wang, Xin Li, Kun Xu, Dongliang He, Qi Zhang, Fu Li, and Errui Ding. Neural color operators for sequential image retouching. In *European Conference on Computer Vision*, pages 38–55. Springer, 2022.
- [31] Yuda Song, Hui Qian, and Xin Du. Starenhancer: Learning real-time and style-aware image enhancement. In *Proceedings of the IEEE/CVF International Conference on Computer Vision*, pages 4126–4135, 2021.
- [32] Hanul Kim, Su-Min Choi, Chang-Su Kim, and Yeong Jun Koh. Representative color transform for image enhancement. In *Proceedings of the IEEE/CVF International Conference on Computer Vision*, pages 4459–4468, 2021.
- [33] Han-Ul Kim, Young Jun Koh, and Chang-Su Kim. Global and local enhancement networks for paired and unpaired image enhancement. In *European Conference on Computer Vision*, pages 339–354. Springer, 2020. 3
- [34] Canqian Yang, Meiguang Jin, Xu Jia, Yi Xu, and Ying Chen. Adaint: Learning adaptive intervals for 3d lookup tables on real-time image enhancement. In *Proceedings of the IEEE/CVF Conference on Computer Vision and Pattern Recognition*, pages 17522–17531, 2022. 3
- [35] Sidi Yang, Bin Xiao Huang, Mingdeng Cao, Yatai Ji, Hanzhong Guo, Ngai Wong, and Yujiu Yang. Taming lookup tables for efficient image retouching. *arXiv preprint arXiv:2403.19238*, 2024.
- [36] Qirui Yang, Peng-Tao Jiang, Hao Zhang, Jinwei Chen, Bo Li, Huanjing Yue, and Jingyu Yang. Learning adaptive lighting via channel-aware guidance. *arXiv preprint arXiv:2412.01493*, 2024. 3
- [37] Michaël Gharbi, Jiawen Chen, Jonathan T. Barron, Samuel W. Hasinoff, and Frédo Durand. Deep bilateral learning for real-time image enhancement. *ACM Transactions on Graphics*, page 1–12, Aug 2017. 3
- [38] Canqian Yang, Meiguang Jin, Yi Xu, Rui Zhang, Ying Chen, and Huaida Liu. Seplut: Separable image-adaptive lookup tables for real-time image enhancement. In *European Conference on Computer Vision*, pages 201–217. Springer, 2022. 3
- [39] Jie Liang, Hui Zeng, and Lei Zhang. High-resolution photo-realistic image translation in real-time: A laplacian pyramid translation network. In *2021 IEEE/CVF Conference on Computer Vision and Pattern Recognition (CVPR)*, Jun 2021. 3
- [40] Yael Pritch, Eitam Kav-Venaki, and Shmuel Peleg. Shift-map image editing. In *2009 IEEE 12th international conference on computer vision*, pages 151–158. IEEE, 2009. 3
- [41] William A Barrett and Alan S Cheney. Object-based image editing. In *Proceedings of the 29th annual conference on Computer graphics and interactive techniques*, pages 777–784, 2002.
- [42] Taeg Sang Cho, Moshe Butman, Shai Avidan, and William T Freeman. The patch transform and its applications to image editing. In *2008 IEEE Conference on Computer Vision and Pattern Recognition*, pages 1–8. IEEE, 2008. 3
- [43] Tim Brooks, Aleksander Holynski, and Alexei A Efros. Instructpix2pix: Learning to follow image editing instructions. In *Proceedings of the IEEE/CVF conference on computer vision and pattern recognition*, pages 18392–18402, 2023. 3, 7
- [44] Bahjat Kawar, Shiran Zada, Oran Lang, Omer Tov, Huiwen Chang, Tali Dekel, Inbar Mosseri, and Michal Irani. Imagic: Text-based real image editing with diffusion models. In *Proceedings of the IEEE/CVF conference on computer vision and pattern recognition*, pages 6007–6017, 2023.
- [45] Manuel Brack, Felix Friedrich, Katharina Kornmeier, Linoy Tsaban, Patrick Schramowski, Kristian Kersting, and Apolinário Passos. Ledits++: Limitless image editing using text-to-image models. In *Proceedings of the IEEE/CVF conference on computer vision and pattern recognition*, pages 8861–8870, 2024.
- [46] Shelly Sheynin, Adam Polyak, Uriel Singer, Yuval Kirstain, Amit Zohar, Oron Ashual, Devi Parikh, and Yaniv Taigman. Emu edit: Precise image editing via recognition and generation tasks. In *Proceedings of the IEEE/CVF Conference on Computer Vision and Pattern Recognition*, pages 8871–8879, 2024. 3
- [47] Chong Mou, Xintao Wang, Jiechong Song, Ying Shan, and Jian Zhang. Diffeditor: Boosting accuracy and flexibility on diffusion-based image editing. In *Proceedings of the IEEE/CVF Conference on Computer Vision and Pattern Recognition*, pages 8488–8497, 2024. 3
- [48] Runze He, Kai Ma, Linjiang Huang, Shaofei Huang, Jialin Gao, Xiaoming Wei, Jiao Dai, Jizhong Han, and Si Liu.

- Freeedit: Mask-free reference-based image editing with multi-modal instruction. *arXiv preprint arXiv:2409.18071*, 2024.
- [49] Qi Mao, Lan Chen, Yuchao Gu, Zhen Fang, and Mike Zheng Shou. Mag-edit: Localized image editing in complex scenarios via mask-based attention-adjusted guidance. In *Proceedings of the 32nd ACM International Conference on Multimedia*, pages 6842–6850, 2024.
- [50] Rahul Sajnani, Jeroen Vanbaar, Jie Min, Kapil Katyal, and Srinath Sridhar. Geodiffuser: Geometry-based image editing with diffusion models. In *2025 IEEE/CVF Winter Conference on Applications of Computer Vision (WACV)*, pages 472–482. IEEE, 2025. 3
- [51] Stephen Batifol, Andreas Blattmann, Frederic Boesel, Saksham Consul, Cyril Diagne, Tim Dockhorn, Jack English, Zion English, Patrick Esser, Sumith Kulal, et al. Flux. 1 kontekst: Flow matching for in-context image generation and editing in latent space. *arXiv e-prints*, pages arXiv–2506, 2025. 3
- [52] Shitao Xiao, Yuezhe Wang, Junjie Zhou, Huaying Yuan, Xingrun Xing, Ruihan Yan, Chaofan Li, Shuting Wang, Tiejun Huang, and Zheng Liu. Omnigen: Unified image generation. In *Proceedings of the Computer Vision and Pattern Recognition Conference*, pages 13294–13304, 2025. 3
- [53] Clément Chadebec, Onur Tasar, Sanjeev Sreetharan, and Benjamin Aubin. Lbm: Latent bridge matching for fast image-to-image translation. *arXiv preprint arXiv:2503.07535*, 2025. 3
- [54] Yang Yang, Siming Zheng, Jinwei Chen, Boxi Wu, Xiaofei He, Deng Cai, Bo Li, and Peng-Tao Jiang. Any-to-bokeh: One-step video bokeh via multi-plane image guided diffusion. *arXiv preprint arXiv:2505.21593*, 2025. 3, 6
- [55] Ziwen Li, Feng Zhang, Meng Cao, Jinpu Zhang, Yuanjie Shao, Yuehuan Wang, and Nong Sang. Real-time exposure correction via collaborative transformations and adaptive sampling. In *Proceedings of the IEEE/CVF Conference on Computer Vision and Pattern Recognition*, pages 2984–2994, 2024. 3
- [56] Yu-Cheng Chiu, Guan-Rong Chen, Zihao Chen, and Yan-Tsung Peng. Abc-former: Auxiliary bimodal cross-domain transformer with interactive channel attention for white balance. In *Proceedings of the Computer Vision and Pattern Recognition Conference*, pages 21258–21266, 2025. 3
- [57] Zhihao Li, Ming Lu, Xu Zhang, Xin Feng, M Salman Asif, and Zhan Ma. Efficient visual computing with camera raw snapshots. *IEEE Transactions on Pattern Analysis and Machine Intelligence*, 46(7):4684–4701, 2024. 6
- [58] Mark D Fairchild. *Color appearance models*. John Wiley & Sons, 2013. 6
- [59] Stephane G Mallat. A theory for multiresolution signal decomposition: the wavelet representation. *IEEE transactions on pattern analysis and machine intelligence*, 11(7):674–693, 2002. 6
- [60] Andrew P Witkin. Scale-space filtering. In *Readings in computer vision*, pages 329–332. Elsevier, 1987. 6
- [61] Shuai Bai, Keqin Chen, Xuejing Liu, Jialin Wang, Wenbin Ge, Sibao Song, Kai Dang, Peng Wang, Shijie Wang, Jun Tang, et al. Qwen2. 5-vl technical report. *arXiv preprint arXiv:2502.13923*, 2025. 6
- [62] Richard Zhang, Phillip Isola, Alexei A Efros, Eli Shechtman, and Oliver Wang. The unreasonable effectiveness of deep features as a perceptual metric. In *Proceedings of the IEEE conference on computer vision and pattern recognition*, pages 586–595, 2018. 7
- [63] Xuemei Zhang, Brian A Wandell, et al. A spatial extension of cielab for digital color image reproduction. In *SID international symposium digest of technical papers*, volume 27, pages 731–734. Citeseer, 1996. 7
- [64] Jack Hessel, Ari Holtzman, Maxwell Forbes, Ronan Le Bras, and Yejin Choi. Clipscore: A reference-free evaluation metric for image captioning. *arXiv preprint arXiv:2104.08718*, 2021. 7
- [65] Nur Muhammad Mahi Shafiullah, Chris Paxton, Lerrel Pinto, Soumith Chintala, and Arthur Szlam. Clip-fields: Weakly supervised semantic fields for robotic memory. *arXiv preprint arXiv:2210.05663*, 2022. 7
- [66] Mathilde Caron, Hugo Touvron, Ishan Misra, Hervé Jégou, Julien Mairal, Piotr Bojanowski, and Armand Joulin. Emerging properties in self-supervised vision transformers. In *Proceedings of the IEEE/CVF international conference on computer vision*, pages 9650–9660, 2021. 7
- [67] Martin Heusel, Hubert Ramsauer, Thomas Unterthiner, Bernhard Nessler, and Sepp Hochreiter. Gans trained by a two time-scale update rule converge to a local nash equilibrium. *Advances in neural information processing systems*, 30, 2017. 7
- [68] Jiangshan Wang, Junfu Pu, Zhongang Qi, Jiayi Guo, Yue Ma, Nisha Huang, Yuxin Chen, Xiu Li, and Ying Shan. Taming rectified flow for inversion and editing. *arXiv preprint arXiv:2411.04746*, 2024. 7
- [69] Black Forest Labs, Stephen Batifol, Andreas Blattmann, Frederic Boesel, Saksham Consul, Cyril Diagne, Tim Dockhorn, Jack English, Zion English, Patrick Esser, Sumith Kulal, Kyle Lacey, Yam Levi, Cheng Li, Dominik Lorenz, Jonas Müller, Dustin Podell, Robin Rombach, Harry Saini, Axel Sauer, and Luke Smith. Flux.1 kontekst: Flow matching for in-context image generation and editing in latent space, 2025. 7, 8
- [70] Zhenxiong Tan, Songhua Liu, Xingyi Yang, Qiaochu Xue, and Xinchao Wang. Ominicontrol: Minimal and universal control for diffusion transformer. In *Proceedings of the IEEE/CVF International Conference on Computer Vision*, pages 14940–14950, 2025. 7

# CameraMaster: Unified Camera Semantic-Parameter Control for Photography Retouching

## Supplementary Material

### 6. More Qualitative Results

We provide additional qualitative comparisons on the CameraSet and Real-world datasets. Fig. 5 to Fig.10 present additional visual comparisons on six photographic retouching tasks: saturation, contrast, film style, exposure, bokeh, and zoom. For each task, we gradually vary the corresponding camera parameter and generate a sequence of outputs. Across all tasks, CameraMaster produces smooth, monotonic, and visually coherent changes in retouching strength, while preserving scene structure, local details, and subject identity. In contrast, compare methods often exhibit non-monotonic behavior, overshooting, or failures to the target setting, and may introduce color cast, banding, or content distortion. These qualitative results further confirm that our semantic-parameter decoupling and joint injection enable precise, interpretable control that balances adherence to the photographic directive with fidelity to the original image.

Fig. 11 shows four representative groups of CameraMaster results on real-world images with joint control over multiple parameters (e.g., exposure, saturation, contrast, and zoom). Our model supports continuous and fine-grained transitions across diverse parameter combinations, yielding natural and consistent retouching effects while maintaining stable geometry and identity. This demonstrates the generality of CameraMaster as a unified camera-centric interface that can realize diverse retouching goals through intuitive, multi-parameter control on real photographic data.

### 7. Effect of content descriptions.

We further study the role of image content descriptions (image captions), as reported in Tab. 4. Removing content descriptions and conditioning only on photographic instructions and camera parameters (*w/o Caption*) leads to a consistent degradation across all metrics: PSNR drops from 32.80 to 29.34, SSIM from 0.9240 to 0.9092, while LPIPS and  $\Delta E$  increase from 0.0669 to 0.0809 and from 3.073 to 4.126, respectively. This shows that content descriptions provide valuable semantic context, enabling better preservation of scene structure and appearance.

At the same time, qualitative results confirm that even without captions, CameraMaster still produces monotonic and consistent retouching along the camera-parameter axis and maintains strong identity preservation. In other words, captions are beneficial but not strictly required: they enhance fidelity and perceptual quality, while the core semantic-parameter alignment remains effective in delivering stable, camera-aware control.

Table 4. Ablation study on content descriptions (image caption). We evaluate the performance on the CameraSet test set.

Settings	PSNR $\uparrow$	SSIM $\uparrow$	LPIPS $\downarrow$	$\Delta E$ $\downarrow$
w/o Caption	29.34	0.9092	0.0809	4.126
Full model	<b>32.80</b>	<b>0.9240</b>	<b>0.0669</b>	<b>3.073</b>

### 8. Limitations and Discussion

Despite its promising results, CameraMaster has several limitations. First, the current implementation supports a maximum resolution of  $1024 \times 1024$ , which restricts its use in high-resolution professional workflows; naive tiling may break global consistency, and scaling to larger resolutions remains future work. Second, although we validate CameraMaster on eight retouching tasks with 38 control levels, the covered functionality is still limited: advanced operations such as shadow, HDR, tone mapping, and relighting are not yet modeled. In addition, our formulation also targets still-image retouching and does not explicitly address temporal consistency in videos or fine-grained, region-specific edits. Finally, the diffusion-based backbone incurs non-trivial computational cost, which can be a bottleneck for latency-sensitive or resource-constrained applications. We leave higher-resolution support, richer control spaces, improved generalization, and more efficient inference as important directions for future work.

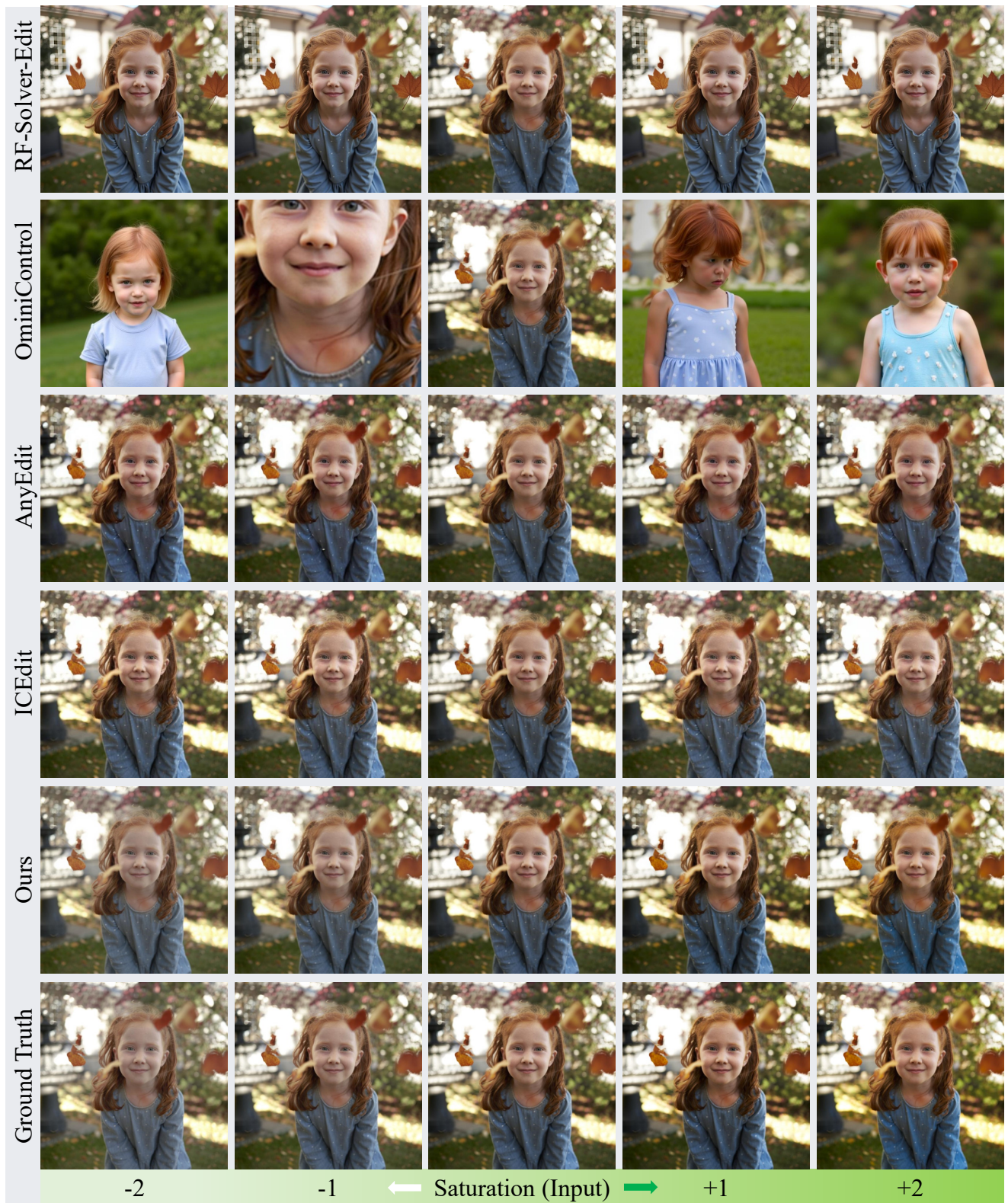


Figure 5. Visual comparison of **Saturation** task retouching results across different methods.

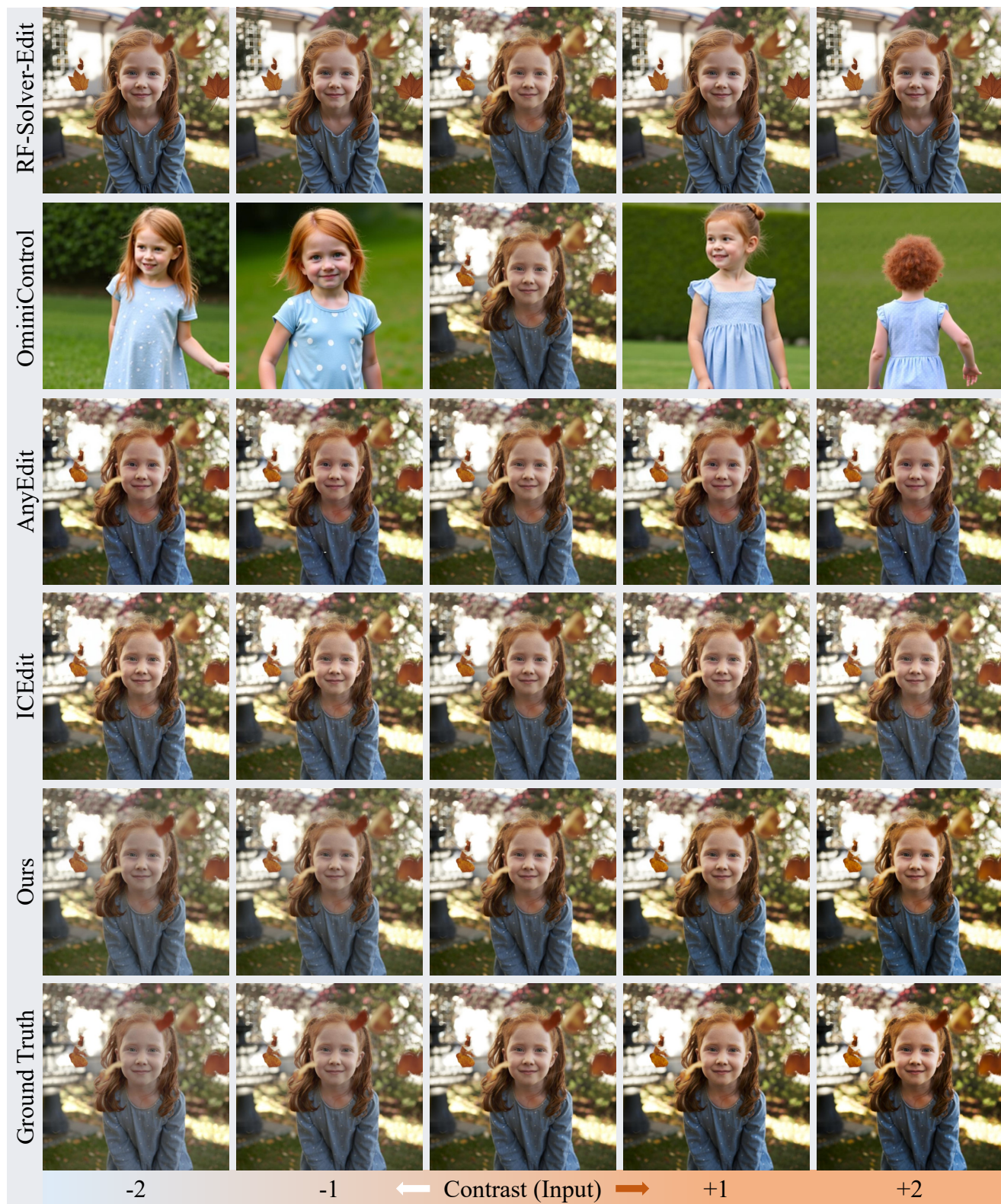


Figure 6. Visual comparison of **Contrast** task retouching results across different methods.

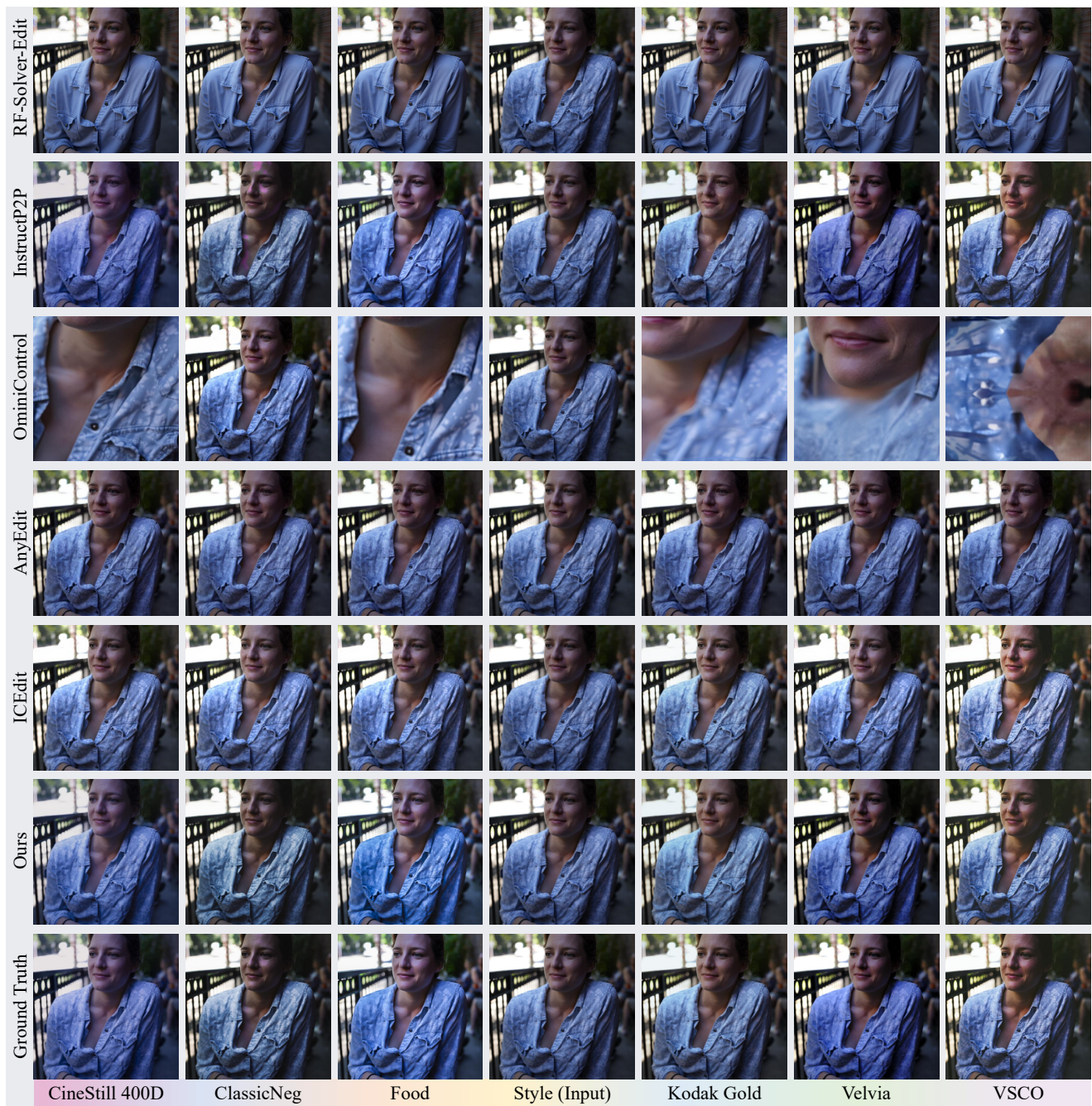


Figure 7. Visual comparison of **Style** task retouching results across different methods.

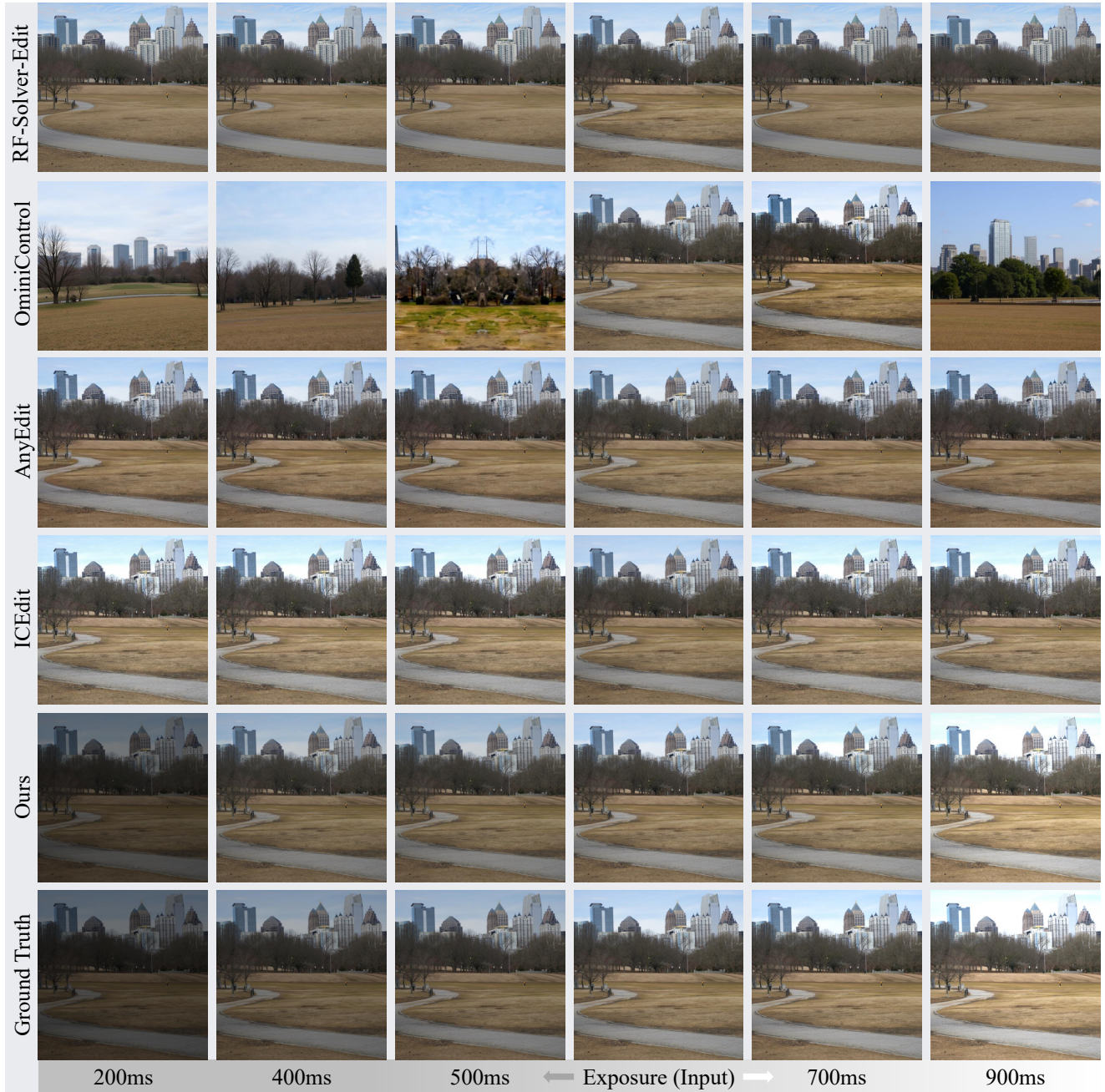


Figure 8. Visual comparison of **Exposure** task retouching results across different methods.

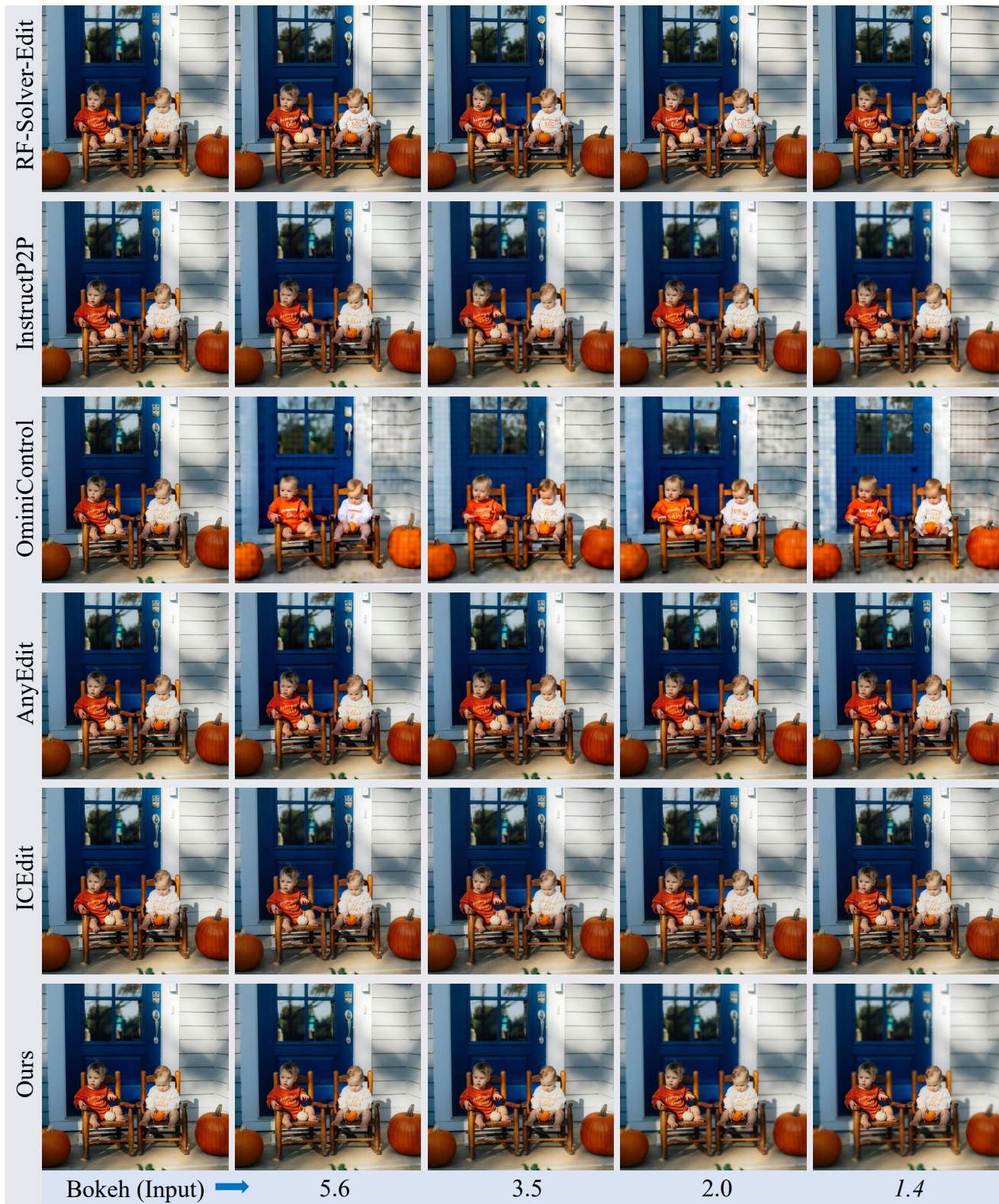


Figure 9. Visual comparison of **Bokeh** task retouching results across different methods.

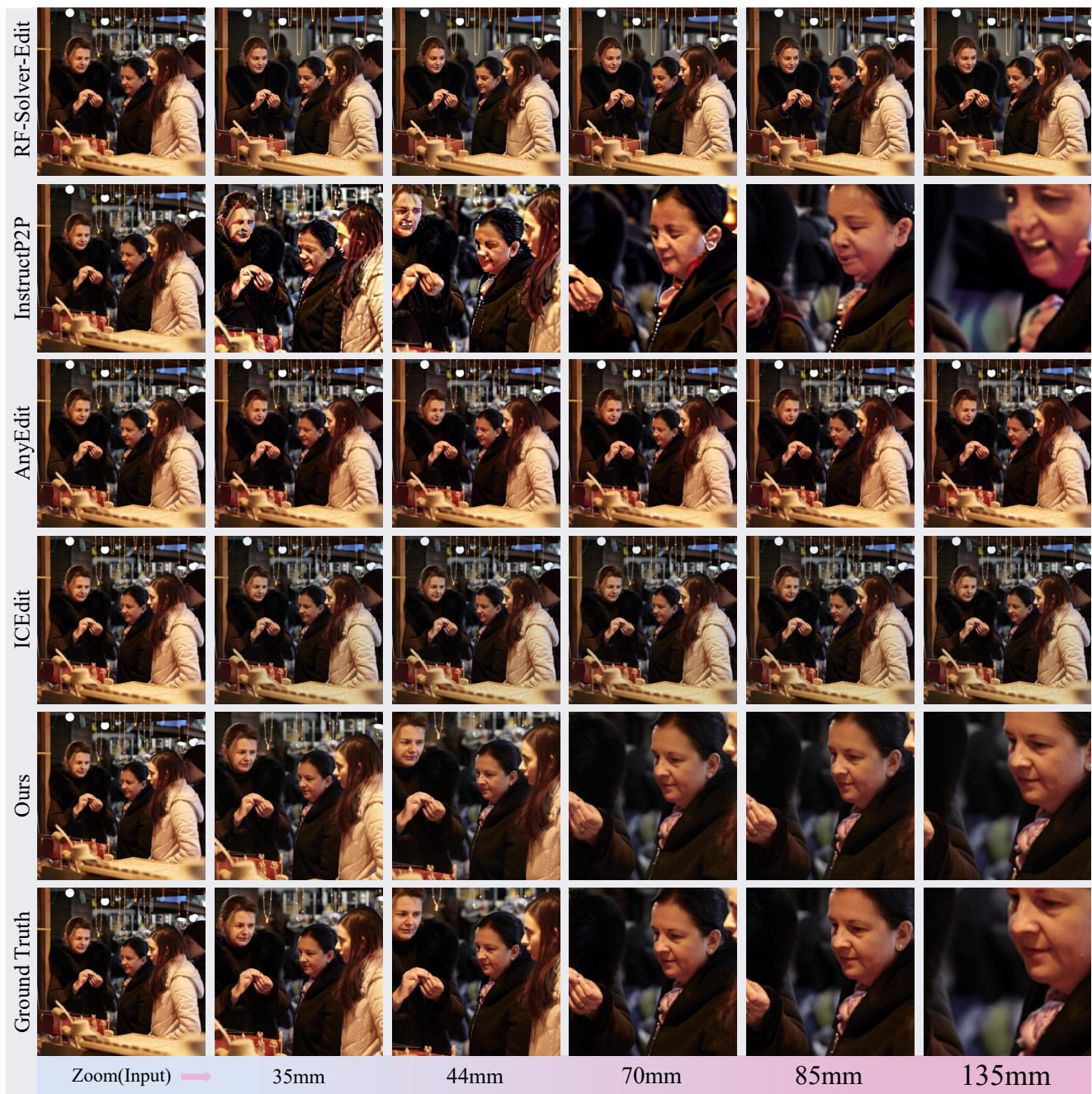


Figure 10. Visual comparison of **Zoom** task retouching results across different methods.

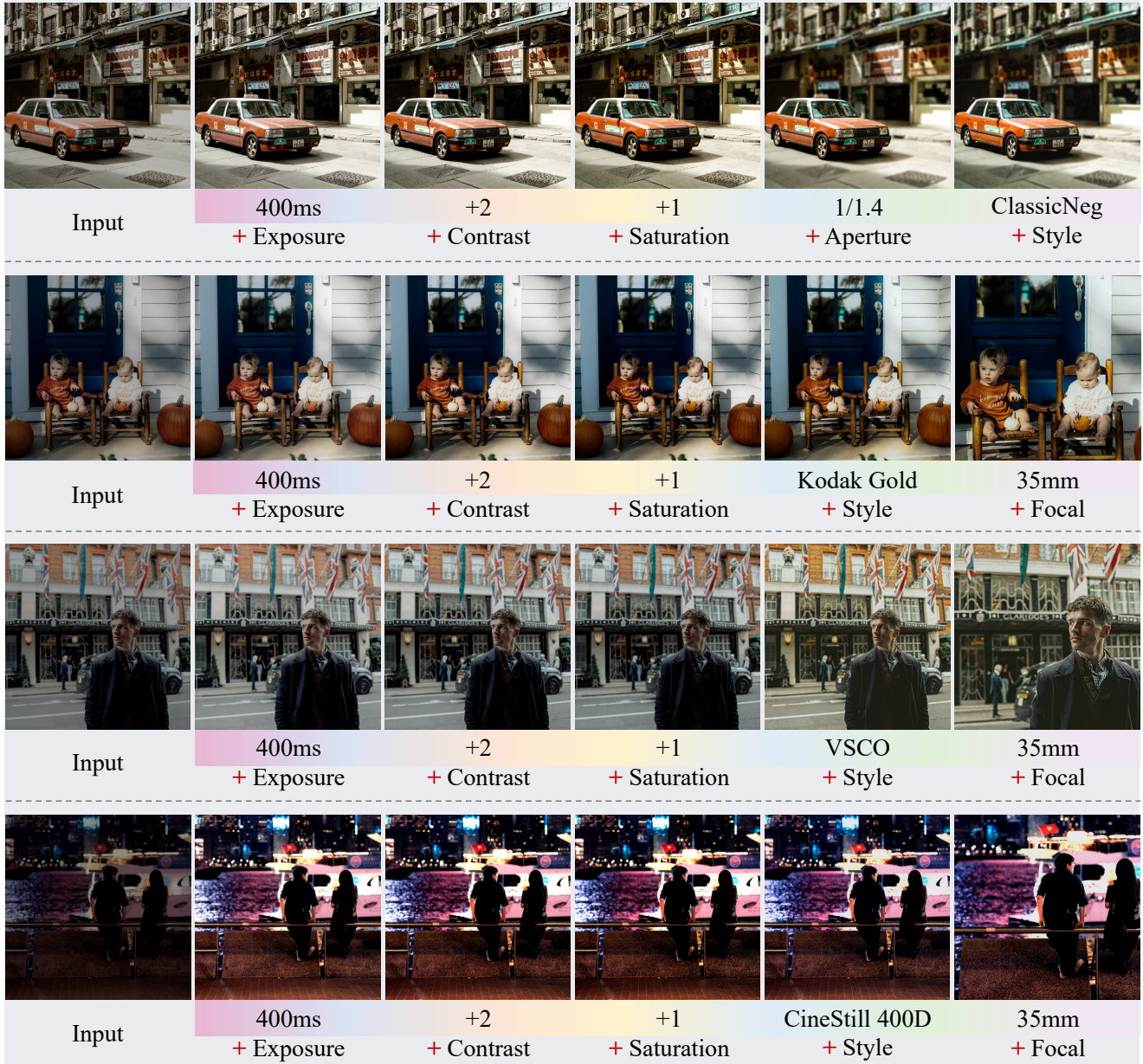


Figure 11. Examples showcase the **cross-parameter** retouching power of CameraMaster on the real-world dataset. Our method enables continuous and fine-grained retouching across multiple parameter combinations, demonstrating CameraMaster’s universal capability in achieving diverse retouching objectives.